The effect of shearing on the onset and vigor of small-scale convection in a Newtonian rheology

Jeroen van Hunen, Jinshui Huang,[1] and Shijie Zhong
Department of Physics, University of Colorado, Boulder, Colorado, USA

Received 4 July 2003; revised 28 August 2003; accepted 3 September 2003; published 8 October 2003.

[1] As an oceanic plate cools with time, the bottom part of the plate may undergo gravitational instabilities and lead to sub-lithospheric small-scale convection (SSC). While numerous previous studies have examined the dynamics of SSC below a fixed top boundary, in this study we investigate the effects of shearing due to plate motion on the onset and time evolution of SSC with 2-D and 3-D finite element models with a prescribed surface plate motion and a Newtonian rheology. Our 3-D models show that plate motion moderately enhances the SSC that displays plate-motion-parallel convective roll-structures. However, plate motion significantly hinders SSC in 2-D models with plate motion that produces plate-motion-perpendicular convective roll-structures. In spite of moderate influences of plate motion on the dynamics of SSC, our results suggest that for Newtonian rheology the onset time of SSC predicted from previous studies with a fixed top boundary is to the first order valid. *INDEX TERMS:* 8120 Tectonophysics: Dynamics of lithosphere and mantle—general; 8121 Tectonophysics: Dynamics, convection currents and mantle plumes; 8155 Tectonophysics: Plate motions—general. **Citation:** van Hunen, J., J. Huang, and S. Zhong, The effect of shearing on the onset and vigor of small-scale convection in a Newtonian rheology, *Geophys. Res. Lett.*, *30*(19), 1991, doi:10.1029/2003GL018101, 2003.

1. Introduction

[2] Cooling oceanic lithosphere may become gravitationally unstable at its base, where a thickening, moderately cold, but not very strong layer is able to detach from the strong part of the lithosphere above. The resulting thermal convection is usually referred to as sub-lithospheric 'small scale convection' (SSC), because of its relatively small wavelengths in comparison with those of tectonic plates. SSC and large-scale convection interfere such that SSC tends to form longitudinal roll (LR) structures (also called 'Richter rolls') of which the axes align with the plate motion direction [*Richter*, 1973; *Richter and Parsons*, 1975]. Based on linear stability analysis [*Richter*, 1973; *Korenaga and Jordan*, 2003a], laboratory experiments [*Richter and Parsons*, 1975], and numerical studies [*Marquart*, 2001], the planform of SSC and the formation and stability of LRs below a moving oceanic lithosphere have been discussed. Many studies have been performed to examine the influence of SSC on the thermal state of the mantle, the surface heat flow, the gravity field, and topography, and results have been applied to estimate the viscosity of the mantle [*Houseman and McKenzie*, 1982; *Yuen and Fleitout*, 1984; *Fleitout and Yuen*, 1984; *Buck and Parmentier*, 1986; *Doin and Fleitout*, 2000].

[3] Onset of SSC below a rigid lid has been studied in both laboratory and numerical studies [*Davaille and Jaupart*, 1993, 1994; *Choblet and Sotin*, 2000; *Korenaga and Jordan*, 2003b; *Huang et al.*, 2003], and scaling laws for the onset time are derived. However, the effect of shearing due to plate motion on SSC has not yet been thoroughly examined. Some 2-D numerical studies have investigated SSC with plate motion [*Houseman*, 1983; *Davies*, 1988; *Dumoulin et al.*, 2001; *Huang et al.*, 2003]. But SSC in these 2-D models display transverse roll (TR) structures (i.e., the axes of the rolls are perpendicular to plate motion), which may be less favorable than LRs with large plate shearing [*Richter and Parsons*, 1975]. A few studies address the effect of plate shearing on the formation rate of LRs [*Richter*, 1973; *Richter and Parsons*, 1975], but only for isoviscous cases, and are not suitable for studying onset time and convective vigor of SSC in the Earth with a strongly temperature-dependent rheology. Extending our understanding on the interaction between plate shearing and LRs requires 3-D modeling, as suggested in [*Huang et al.*, 2003] and [*Korenaga and Jordan*, 2003a].

[4] Here, we examine the effect of shearing from a moving plate on the onset time and vigor of SSC for both TRs and LRs with 2-D and 3-D models with realistic rheology. Although linear stability analysis indicates that LRs should be unaffected by background shearing [e.g., *Korenaga and Jordan*, 2003a and references therein], such analysis may not completely apply to the situation with fully developed convective regime. We address the basic question whether and how large scale shearing affects the onset and vigor of SSC in a 3-D geometry, and compare results to 2-D models with shearing and TRs, or without shearing.

2. Model Setup

[5] To study SSC, we applied an incompressible fluid model in 2-D and 3-D with infinite Prandtl-number and Boussinesq approximations, using the finite element code Citcom [*Moresi and Gurnis*, 1996; *Zhong et al.*, 2000]. Non-dimensional governing equations are given as:

$$\nabla \cdot \mathbf{u} = 0, \tag{1}$$

$$-\nabla \cdot P + \nabla \cdot \left[\eta\left(\nabla \mathbf{u} + \nabla^T \mathbf{u}\right)\right] + \mathrm{Ra}T\mathbf{e}_z = 0, \tag{2}$$

$$\frac{\partial T}{\partial t} + \mathbf{u} \cdot \nabla T = \nabla^2 T, \tag{3}$$

[1]Now at Department of Geophysics, School of Geodesy and Geometrics, Wuhan University, Wuhan, P.R. China.

0094-8276/03/2003GL018101$05.00

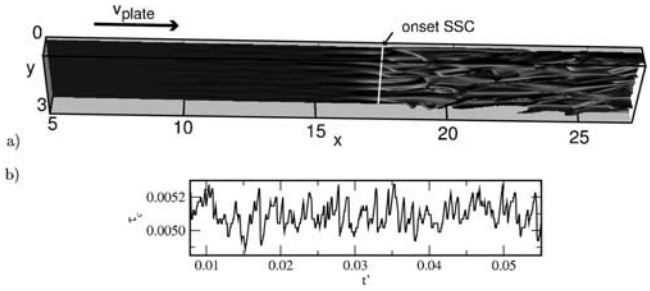

Figure 1. 3-D SSC model results for Ra = 5×10^7, θ = 7.42, and *Pe* = 3608. a) A snapshot of thermal structure (isosurface of $T = 0.95$), viewed from below, shows the onset and longitudinal roll-structure of SSC in a 3-D model with plate motion. b) The time-dependent onset time of SSC τ_c versus the model time t'.

with **u**, P, η, T, and $\mathbf{e}_z$ the non-dimensional velocity vector, pressure, viscosity, and temperature, and the vertical unit vector, respectively. $\mathrm{Ra} = \frac{\alpha\rho_0 g\Delta T h^3}{\kappa\eta_0}$ is the Rayleigh number, with α the thermal expansion coefficient, ρ_0 the reference mantle density, g the gravitational acceleration, ΔT and h the temperature difference across and height of the model domain, κ the thermal diffusivity, and η_0 the reference viscosity at $T = 1$ and, in case of rheological layering, the top layer. A linear Arrhenius viscosity equation is used:

$$\eta = \eta_b/\eta_0 \exp\left(\frac{E}{T + T_{\mathrm{off}}} - \frac{E}{1 + T_{\mathrm{off}}}\right) \tag{4}$$

In this equation, η_b equals η_0 except for the case of stratified rheology, for which η_b is explicitly described. $E = E^*/(R\,\Delta T)$ is the scaled equivalent of the activation energy E^*, and T_{off} is the non-dimensional surface temperature. The following characteristic scales were used for non-dimensionalization: length scale h, time scale h^2/κ, viscosity scale η_0, and temperature scale ΔT. Non-dimensional model parameters are used throughout the paper, but for comparison, dimensional equivalents are sometimes given, using $\alpha = 3 \times 10^{-5}$ K^{-1}, $\rho_0 = 3300$ kg/m^3, $g = 9.8$ m/s^2, $\Delta T = 1350$ K, $h = 1000$ km, and $\kappa = 10^{-6}$ m^2/s.

[6] Here, three different models are defined to study SSC. In 2-D, a model with the vertical model plane perpendicular to plate motion produces SSC with longitudinal rolls (LRs) [*Richter*, 1973]. A 2-D model plane parallel to plate motion produces SSC with transverse rolls (TRs). A 3-D model is necessary to examine the 3-D convective structures of SSC, and to study the shearing effect of plate motion on LRs. Here, our focus is on 2-D TR models and 3-D models, while 2-D LR results are taken from *Huang et al.* [2003]. We compare results from each of these models.

[7] The 2-D LR calculations from [*Huang et al.*, 2003] were performed in a box with aspect ratio 3 with a no-slip top at $T = 0$, free-slip $T = 1$ conditions at the bottom, and an initial $T = 1$ everywhere in the box, which corresponds to a zero-age lithosphere. The 2-D TR and 3-D calculations presented here are performed in a model domain with an aspect ratio a varying between 3 and 42 in x-direction (the direction of plate motion), while for 3-D models, the width of the box (i.e., perpendicular to plate motion, see Figure 1) is fixed to 3. The large aspect ratio models are used for calculations with large plate motion. The top boundary has a prescribed velocity v_{plate} in positive x-direction, which is non-dimensionalised to a Peclet number $\mathrm{Pe} = v_{plate}h/\kappa$, and the bottom has a no-slip boundary condition. $T = 0$ and 1 at the top- and bottom boundaries, respectively. Flow-through boundaries are present at $x = 0$ and $x = a$, and side boundaries at $y = 0$ and $y = 3$ are reflecting. Inflow velocity corresponds to a Couette flow for given viscosity profile and top and bottom boundary velocities. The inflow temperature corresponds to a non-dimensional lithospheric age $t_0 = 1.58 \times 10^{-4}$ (or 5 Ma). At model time $t' = 0$, a cooling halfspace temperature field, corresponding to the inflow age and plate velocity, is prescribed in the total model domain. Schematic representations of the 2-D LR, 2-D TR, and 3-D models are shown in [*Huang et al.*, 2003, Figure 1].

[8] A relative random temperature perturbation $\epsilon = [-10^{-3}, 10^{-3}]$ (which differs from the purely positive $\epsilon = [0, 10^{-3}]$ in *Huang et al.* [2003]) is added to the temperature field. For the 2-D LR models, this perturbation is added to the initial condition, while for 2-D TR and 3-D models, it is added at the inflow boundary throughout the calculation. Calculations are performed until a statistically steady state thermal situation is reached.

[9] The onset time τ_c of small-scale convective instabilities in 2-D TR models is defined as the age of the lithosphere at which the temperature at any depth starts to deviate from the cooling halfspace solution by more than 1%. In 2-D LR models, the horizontally averaged temperature was used to determine τ_c [*Huang et al.*, 2003], and 3-D models use the y-averaged temperature. Different τ_c-measurements for the different models (2-D LR, 2-D TR, and 3-D) are inevitable, but resulting uncertainties in τ_c are small enough to allow for a first-order comparison between results from these three models. Note that in the 2-D TR and 3-D models, the lithospheric age is given by $t_0 + x/\mathrm{Pe}$.

3. Onset Time and Convective Vigor of SSC

[10] We determine the influence of shearing from surface motion on the underlying SSC by comparing onset time and convective vigor of SSC instabilities for 2-D TR models and 3-D models with results from LR models (i.e., with a static plate).

[11] We start with a comparison of SSC onset times. For 2-D LR models, the SSC onset time τ_c is described by the following scaling law [*Huang et al.*, 2003]:

$$\tau_c = A\mathrm{R}a^{-0.68}\theta^{0.74}, \tag{5}$$

in which $\theta = E/(1 + T_{off})^2$ is the Frank-Kamenetskii parameter for unit non-dimensional internal temperature [*Solomatov and Moresi*, 2000]. The prefactor $A = 60.6$ differs slightly from the one by [*Huang et al.*, 2003] due to different definition of ϵ. Because this scaling law was developed for a depth-independent viscosity, we use the same viscosity equation (4) as in *Huang et al.* [2003] for models in this section.

[12] Figure 1 illustrates the 3-D SSC development with Ra = 5×10^7, θ = 7.42 (E^* = 120 kJ/mol), and *Pe* = 3608 (~11 cm/yr). The relatively low value for E^* corresponds to an estimate by [*Watts and Zhong*, 2000], and is used to approximate the expected (additional) effect from disloca-

tion creep [*Christensen*, 1984]. The young lithosphere (at small x) remains stable, and does not show any convective behavior. At a certain age, SSC starts and sheet-like downwellings parallel to the plate motion develop. For larger age, fully developed convective rolls have their axes parallel to the plate motion [*Richter*, 1973] (Figure 1a). Due to intrinsic randomness, the exact τ_c varies over a few percent through time (Figure 1b). We performed a set of 3-D model calculations to determine τ_c, and compared results with those from the scaling law in Equation (5) for the 2-D LR model. Results are shown in Figure 2 for a range of (non-dimensional) plate velocities Pe, for Rayleigh numbers Ra = 5×10^6, 10^7, and 5×10^7, and θ = 7.42 and 14.84 (corresponding to E^* = 120 and 240 kJ/mol). To first degree, τ_c for the 3-D models agrees with the scaling law results for 2-D LR models with no plate shearing. However, the plate-velocity has a moderate and systematic influence on τ_c: larger plate motion gives smaller onset times.

[13] For the same Ra and θ, onset is also calculated for SSC in 2-D TR models. Figure 2 shows that for these models, τ_c is considerably more sensitive to plate motion. All calculations show a rapid increase of τ_c with Pe for large enough Pe. This indicates that in 2-D, SSC onset can be significantly delayed by plate motion. Figure 2 further indicates that the smaller the onset time τ_c is, the larger Pe should be in order to influence τ_c in the 2-D TR model. For Ra = 5×10^7 and θ = 7.42 (or E^* = 120 kJ/mol), v_{plate} > 10 cm/yr is needed to influence τ_c in the 2-D TR model.

[14] Next, we study the influence of shearing on the evolution of SSC. A more realistic depth-dependent viscosity was used here, because it may have significant effects on fully developed SSC [*Robinson and Parson*, 1988]. 2-D TR and 3-D calculations are performed for $Ra = 5 \times 10^7$, and θ = 11.1 (or E^* = 180 kJ/mol). We increased the relative viscosity η_b of the transition zone (below 410 km depth) and lower mantle (below 660 km depth) to η_b = 19.09 (corresponding to a viscosity of 5×10^{20} Pa s for T = 1350°C) and η_b = 190.9 (5×10^{21} Pa s), respectively. The stratified viscosity may enhance the effect of plate shearing. We monitor the vigor of SSC with the vertical root-mean-square velocity $v_{z,rms} = \sqrt{\int_{d_1}^{d_2} v_z^2 dz/(d_2 - d_1)}$ over a dimensionless depth range z = [0.6,0.85] in which SSC occurs (with the surface defined as z = 1), gathered in $\Delta t = 1.58 \times 10^{-4}$ (or 5 Ma) lithospheric age 'bins'. To deal with the intrinsic variability of SSC, $v_{z,rms}$ is further averaged over model time t, and in y-direction for 3-D models.

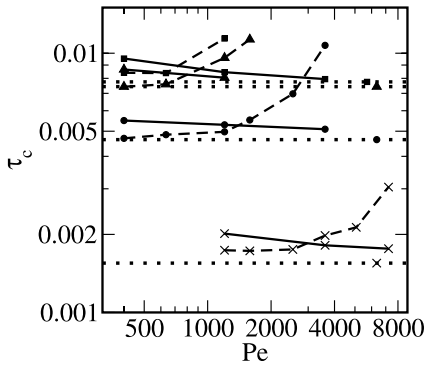

Figure 2. Relation between onset time τ_c and non-dimensional plate velocity Pe for 3-D models (solid lines), 2-D TR models (dashed lines), and scaling law values from *Huang et al.* [2003] for 2-D LR models with no plate motion (straight dotted lines). Model parameters: Ra = 5×10^6, θ = 7.42 (triangles); Ra = 10^7, θ = 14.9 (squares); Ra = 10^7, θ = 7.42 (circles); and Ra = 5×10^7, θ = 7.42 (crosses). All 3-D calculations show a moderate decrease of τ_c with increasing Pe, while for 2-D LR models, τ_c increases rapidly for large enough Pe.

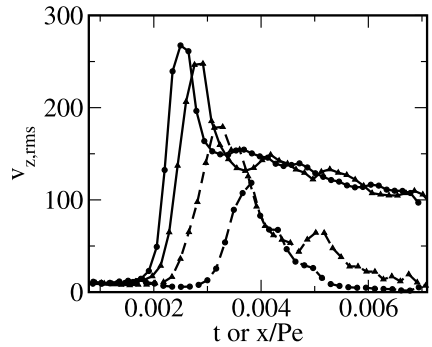

Figure 3. Vertical rms velocity $v_{z,rms}$ versus lithospheric age t for model calculations with Ra = 5×10^7, θ = 11.1, and a depth-dependent viscosity (see text) in 3-D (solid lines) and 2-D TR (dashed lines) for Pe = 1585 (triangles) and 2537 (circles). In 2-D TR models, $v_{z,rms}$ peaks at increased age with reduced amplitude as Pe increases, while for 3-D models, the effects of Pe on $v_{z,rms}$ are opposite.

[15] Figure 3 shows $v_{z,rms}$ for Pe = 1585 and 2537 (or v_{plate} = 5 and 8 cm/yr). For those calculations, $v_{z,rms}$ is negligibly small for young lithosphere, consistent with the absence of SSC. Around τ_c, $v_{z,rms}$ rapidly increases to a peak value, after which it slowly decreases. This peak in $v_{z,rms}$ reflects the first SSC instability, which is more vigorous than later ones. Again, a few fundamental differences between 2-D TR and 3-D calculations can be observed. SSC stops for large lithospheric age in the 2-D TR calculation with high Pe. This is illustrated more clearly in Figure 4, where the thermal structure and $v_{z,rms}$ for one snapshot indicate the presence of SSC over a limited lithospheric age-range. In 3-D models, $v_{z,rms}$ also reduces after the onset of SSC, but remains significant for all ages after the onset (Figure 3). The effect of increasing plate velocity differs for 2-D and 3-D: first, it delays the onset in 2-D, but moderately enhances the onset in 3-D, consistent with the results in Figure 2t. Second, the vigor of SSC is reduced with increasing plate shear in 2-D, but increases with shear in 3-D.

4. Discussion and Concluding Remarks

[16] When SSC occurs in a mantle with moving plates, longitudinal rolls (LRs) may be dominant over transverse ones (TRs). We have performed numerical calculations to examine the influence of shear by moving plates on the onset time and vigor of small-scale convection for both LRs and TRs. Our results show that shearing significantly delays the onset of TRs, and reduces their vigor, and in some cases almost even eliminates them. For LRs, the effect is smaller and opposite: onset time decreases, and convective vigor increases with increasing shear. This indicates that shearing

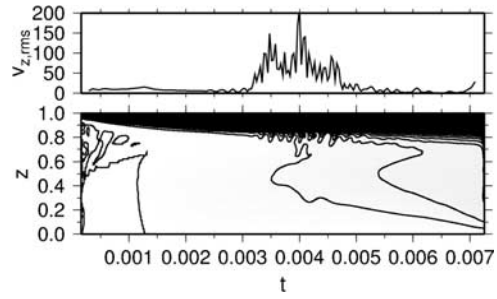

Figure 4. a) A snapshot of vertical rms velocity $v_{z,rms}$ versus lithospheric age t and b) contour plot of the temperature field with 0.02 temperature isotherm intervals for the 2-D TR model with Pe = 2537 from Figure 3. Here, $v_{z,rms}$ is not averaged over age bins.

has a moderate influence on LRs, which is different from linear stability analysis predictions. Nonetheless, considering the intrinsic fluctuation of SSC onset time, and uncertainties from measurement differences, the onset of SSC from 2-D LR models with a fixed top is to first order consistent with more realistic 3-D model results with plate motion.

[17] A few previous studies have examined the shearing effect on SSC. The delay in SSC onset due to shearing in 2-D TR models was reported before for isoviscous thermal convection by *Houseman* [1983], who showed that the critical boundary Rayleigh number increases with increasing Peclet number. *Huang et al.* [2003] also reported such delay for a limited range of plate motions. However, our results show that the shearing effect in 3-D models is opposite to that in 2-D TR models. Understanding the physics that is responsible for this difference will be topic of future studies.

[18] For large shear, our 2-D TR models show that SSC with TRs only develop over a limited age range (Figures 3 and 4). The switch-off of SSC at large age is most likely caused by the increased shear below an old plate that may become large enough to suppress TR SSC completely. As the lithosphere grows thicker (despite the presence of SSC), the underlying asthenosphere becomes thinner, and the shear stress induced by the large-scale plate motion increases. Figure 4 further indicates that the temperature below old lithosphere decreases due to the cooling effect of SSC, which locally increases the viscosity and therefore the shear. *Huang et al.* [2003] illustrated that the asthenospheric thickness influences SSC, even without shearing. If this thickness becomes comparable to the wavelength of the SSC convective instabilities, the local Rayleigh number for the convective instability is reduced. However, because switch-off of SSC occurs only for 2-D TR models with large plate motion, shearing is a more likely explanation.

[19] The models in this paper all consider Newtonian rheology. Non-Newtonian rheology will influence onset time and vigor of convection through a different physical mechanism. Mantle flow and plate motion create a shear stress that affects the effective viscosity, and therefore the effective Rayleigh number, which, in turn, influences SSC onset time (Equation 5), and convective vigor. SSC may itself change the ambient shear stress, and the resulting nonlinear feedback mechanism may create a complicated (possibly oscillatory [*Fleitout and Yuen*, 1984]) relation between SSC and the ambient shear stress, for which LRs are not necessarily the preferred structure [*Schmeling*, 1987]. The effects of non-Newtonian rheology on the dynamics of SSC in 3-D models will be a subject of future research.

[20] **Acknowledgments.** This study is funded by David and Lucile Packard Foundation and NSF under Grant number EAR 0134939. The authors appreciate constructive reviews by Sarah Zaranek and Slava Solomatov.

References

Buck, W. R., and E. M. Parmentier, Convection beneath young oceanic lithosphere: Implications for thermal structure and gravity, *J. Geophys. Res.*, *91*, 1961–1974, 1986.

Choblet, G., and C. Sotin, 3D thermal convection with variable viscosity: Can transient cooling be described by a quasi-static scaling law?, *Phys. Earth Planet. Inter.*, *119*, 321–336, 2000.

Christensen, U. R., Convection with pressure and temperature dependent non-Newtonian rheology, *Geoph. J. R. Astron. Soc.*, *77*, 242–284, 1984.

Davaille, A., and C. Jaupart, Transient high-Rayleigh-number thermal convection with large viscosity variations, *J. Fluid Mech.*, *253*, 141–166, 1993.

Davaille, A., and C. Jaupart, Onset of thermal convection in fluids with temperature-dependent viscosity: Application to the oceanic mantle, *J. Geophys. Res.*, *99*, 19,853–19,866, 1994.

Davies, G. F., Ocean bathymetry and mantle convection 2. small-scale flow, *J. Geophys. Res.*, *93*, 10,481–10,488, 1988.

Doin, M.-P., and L. Fleitout, Flattening of the oceanic topography: Thermal versus dynamic origin, *Geophys. J. Int.*, *143*, 582–594, 2000.

Dumoulin, C., M. P. Doin, and L. Fleitout, Numerical simulation of the cooling of an oceanic lithosphere above a convective mantle, *Phys. Earth Planet. Inter.*, *125*, 45–64, 2001.

Fleitout, L., and D. A. Yuen, Secondary convection and the growth of the oceanic lithosphere, *Phys. Earth Planet. Inter.*, *36*, 181–212, 1984.

Houseman, G. A., Large aspect ratio convection cells in the upper mantle, *Geoph. J. R. Astron. Soc.*, *75*, 309–334, 1983.

Houseman, G. A., and D. P. McKenzie, Numerical experiments on the onset of convective instability in the Earth's mantle, *Geoph. J. R. Astron. Soc.*, *68*, 133–164, 1982.

Huang, J., S. Zhong, and J. van Hunen, Controls on sub-lithospheric small-scale convection, *J. Geophys. Res.*, *108*(B8), 2405, doi:10.1029/2003JB002456, 2003.

Korenaga, J., and T. H. Jordan, Physics of multi-scale convection in the Earth's mantle. Evolution of sublithospheric convection, *J. Geophys. Res.*, in press, 2003a.

Korenaga, J., and T. H. Jordan, Physics of multi-scale convection in the Earth's mantle, Onset of sublithospheric convection, *J. Geophys. Res.*, *108*(B7), 2333, doi:10.1029/2002JB001760, 2003b.

Marquart, G., On the geometry of mantle flow beneath drifting lithospheric plates, *Geophys. J. Int.*, *144*, 356–372, 2001.

Moresi, L., and M. Gurnis, Constraints on the lateral strength of slabs from three-dimensional dynamic flow models, *Earth Plan. Sci. Let.*, *138*, 15–28, 1996.

Richter, F. M., Convection and large-scale circulation of the mantle, *J. Geophys. Res.*, *78*, 8735–8745, 1973.

Richter, F. M., and B. Parsons, On the interaction of two scales of convection in the mantle, *J. Geophys. Res.*, *80*, 2529–2541, 1975.

Robinson, E. M., and B. Parson, The effects of a shallow low-viscosity zone on small-scale instabilities under the cooling oceanic plates, *J. Geophys. Res.*, *93*, 3469–3479, 1988.

Schmeling, H., On the interaction between small- and large-scale convection and postglacial rebound flow in a power-law mantle, *Earth Plan. Sci. Let.*, *84*, 254–262, 1987.

Solomatov, V. S., and L. N. Moresi, Scaling of time-dependent stagnant convection: Application to small-scale convection on Earth and other terrestrial planets, *J. Geophys. Res.*, *105*, 21,795–21,817, 2000.

Watts, A. B., and S. Zhong, Observations of flexure and the rheology of oceanic lithosphere, *Geophys. J. Int.*, *142*, 12,177–12,190, 2000.

Yuen, D. A., and L. Fleitout, Stability of the oceanic lithosphere with variable viscosity: An initial-value approach, *Phys. Earth Planet. Inter.*, *34*, 173–185, 1984.

Zhong, S., M. T. Zuber, L. Moresi, and M. Gurnis, Role of temperature-dependent viscosity and surface plates in spherical shell models of mantle convection, *J. Geophys. Res.*, *105*, 11,063–11,082, 2000.

J. van Hunen, J. Huang, and S. Zhong, Department of Physics, University of Colorado at Boulder, Campus Box 390 Boulder, CO 80309-0390, USA. (hunen@colorado.edu)